

Some Results of Spectral and Radiative Measurements During IOP - 1996 in Tomsk

V. V. Zuev, B. D. Belan, V. P. Galileiskii, S. I. Dolgii, V. S. Kozlov, V. N. Marichev,
A. M. Morozov and V. K. Oshlakov
*Institute of Atmospheric Optics
Russian Academy of Sciences
Tomsk, Russia*

Introduction

At present the problems of the radiation transfer theory in the cloudy atmosphere have not been completely developed. However, a series of problems is available, which can be solved only as a result of complex experimental measurements of spectral, radiation, thermodynamic, microphysical, and other characteristics of cloudiness. In particular, cloudiness is a readily scattered and absorbed polydisperse system characterized by an essential inhomogeneity both in vertical and in horizontal directions; cloudiness is also characterized by a variety of optical and microphysical parameters. Because of this, the complex measurements in the free atmosphere are of particular significance.

Experiment

In September - November 1996 in the framework of the ARM - 96 program in the Tomsk region, measurements were made of spectral dependencies of direct and scattered solar radiation for various atmospheric conditions, namely, clear sky, translucidus of upper cloud level (through which the sun can be observed); opacus clouds of the middle and upper clouds (the sun cannot be observed).

To record the spectra of direct solar radiation, the following instruments are used: a stellar - solar photometer based on a telescope AZT - 7 ($d=200\text{mm}$, $f=2000\text{mm}$), with interference filters for wavelengths of 420, 530, 690 and 780nm, $\Delta\lambda=10\text{nm}$ (A. Abramochkin et al. 1981); a sun photometer-heliostat with angular aperture of 1° providing the recording of light flows in the wavelength range of 300 - 600nm with the average resolution of 3nm, the time for recording one spectrum is 2 min. For recording the direct and scattered solar radiation, a sun spectrophotometer is used based on a monochromator MDR - 23 (the spectral range is 400 - 700nm, the spectral resolution is 5nm, the time for spectral recording is 1m), but a shadow aureole photometer (combined with CCD-matrix) is used when observing the scattered solar

radiation in the space about the sun. Simultaneously, with spectral observations, we observe the spectral integral solar radiation fluxes using a pyranometer (400 - 2300nm) and a meter of radiation balance (400 - 14000nm).

Results and Discussion

During the experiments carried out in fall 1996, we have obtained more than 400 spectra of the direct solar radiation in the 400 to 700 nm range, and more than 200 spectra of scattered solar radiation. The values of the solar brightness outside the atmosphere are estimated based on the results of observations of direct solar radiation using a stellar - solar photometer (on the basis of the "long Bouguer method"). When processing the results of observations, the following parameters are analyzed: the spectral optical depths normalized to the unit air mass, and spectral fluxes of direct and scattered solar radiation normalized to the solar spectrum outside the atmosphere; color temperature and the pseudograyness factor of the space about the sun (V. Galileiskii et al. 1994); and color coordinates (V. Oshlakov 1990) calculated on the basis of spectral fluxes of direct solar radiation.

Color Temperature and the Pseudograyness Factor

Figure 1 shows the pseudograyness index distribution for the red spectral range in the space about the sun, obtained on September 10, 1996, at the sun culmination. The initial data of the shadow aureole photometer are processed by the skeleton diagram method, one of the traditional methods of description, analysis and shape transformation of screen and continuous images (Serra 1981). The index minimum values are denoted by black and the maximum values by white; the intermediate values in Figure 1 are given with the step 10 in the range from 0 to 256.

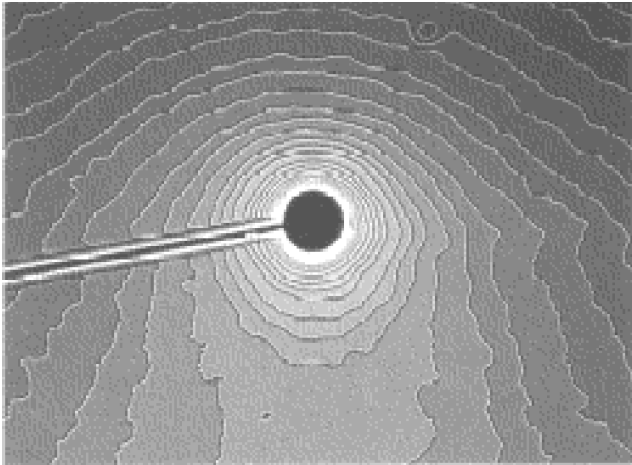


Figure 1. Pseudograyness index distribution for red spectral range in space about the sun.

During observations with the use of the stellar-solar photometer the atmospheric transparency is checked. Its values normalized to zenith for $\lambda = 0.53 \mu\text{m}$ are about 0.82. Figure 1 shows the solar screen with an angular size about 1° . Analysis of this figure shows that the distribution of values of the pseudograyness index is of symmetric nature for the solar meridian. Maximum values of the above-mentioned index are observed directly near the sun, and minimum values are observed when moving from the sun to the circumzenithal area.

Figure 2 shows the results of calculations of the values of the color temperature index obtained for the same conditions of observation (with the same step of 10 in the range of values from 0 to 256). In this case, the color temperature of the sun corresponds to minimum values of the color temperature index (black). Joint analysis of the above results makes it possible to select the four areas where the pronounced peculiarities are available in the brightness level and in the spectral brightness distribution

- In the range from 0.5° to 2° , directly near the sun as a result of interaction of solar radiation with atmospheric particles, a bright airglow occurs. Its spectrum is similar to the solar spectrum (the index of the color temperature here is low).
- The spheric-solar path, situated under the sun in its meridian, is also a bright observed object with the spectrum similar to the solar spectrum; the values of the color temperature index here are also small.

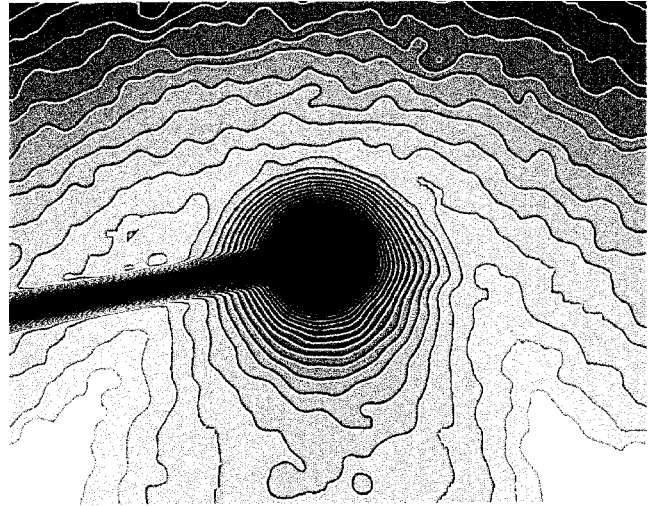


Figure 2. Results of calculations of values of color temperature index for same condition of observation.

- An arc encircled the sun and the atmospheric-solar path; brightness of this arc is not large, but exactly in this area the radiation spectrum has an essential rise in short-wave part. Here the values of the color temperature index reach their maximum.
- In this area, covering from above all the three preceding ones, the low values of the above indexes are observed.

Direct and Scattered Solar Radiation

Radiation fluxes obtained under cloudless conditions, at dense continuous and low-level cloudiness, and at high-level continuous cloudiness are presented at Figure 3. There is a monotonous decrease in the flux observed at increasing wavelength for the case of the scattering in air. The ratio of the fluxes at 400 and 700 nm is 2.5 to 2.7. There is a fine structure superimposed on the monotony fall off of the spectral curve. Thus one can identify the minima at 465, 550, 580, and 680 nm, and as a whole, a distinct fall off between 550 to 650 nm. When considering upper curves in Figure 3, which describe the scattering in continuous clouds, we can see that they have similar fine spectral structure as it is observed in cloudless conditions. But in contrast to the latter case, its structure is more pronounced and its absolute amplitude is larger by several times; however, their relative amplitudes are approximately equal. Furthermore, there is no trend observed toward monotonic decrease of the spectral flux from these curves.

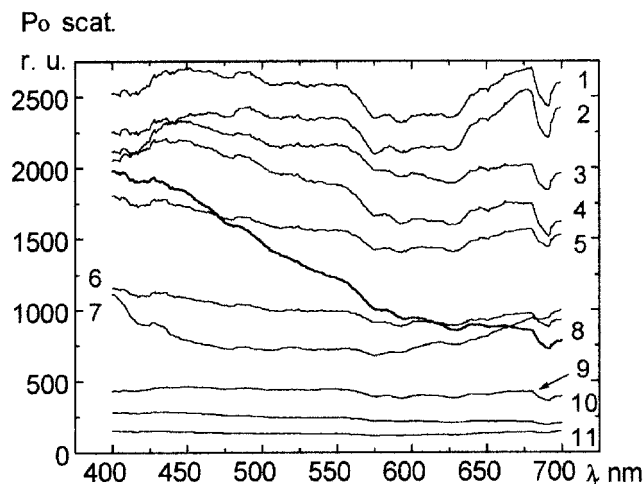


Figure 3. Spectrum of normalized flux of the solar radiation scattered in clear sky conditions (8), and the presence of continuous translucent clouds(1-5), and low-level continuous dense clouds (6,7,9,10). (1-10/Cs fib, haze strong; 2-10/Sc trans; 3-9/Ac und; 4- 10/Sc; 5-10/Ac floc, Sc und 6-7; 6-10/Sc trans; 7-10/Sc op; 8-0/0; 9-10/Sc, St; 10-10/St; 11-Sc und.)

The neutral behavior of the spectral curve is especially well seen for the dense continuous cloudiness. At the same time, the fine spectral structure is practically blurred. Spectral fluxes for the conditions of broken cloudiness (cloud fraction about 6) are presented in Figure 4.

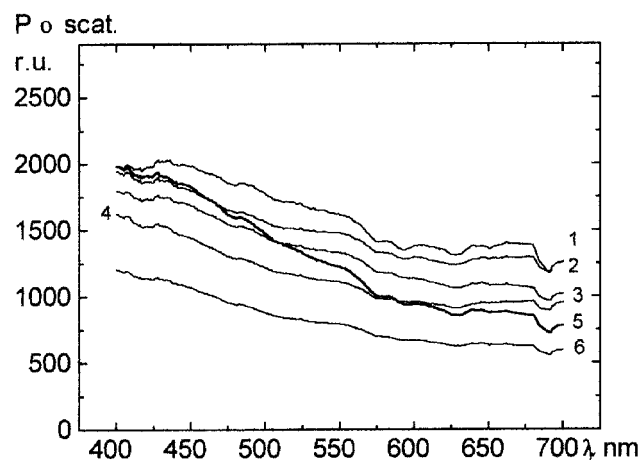


Figure 4. Spectra of normalized flux of the solar radiation scattered in the presence of broken cloudiness. (1-1/Ci; 2-2/Ci fil-6/Cs neb; 3- Cu hum; 4- 3/Ac und; 5-0/0; 6- 2/Ac cuf, haze thin.)

Here, an insignificant decrease of spectral flux is observed with the wavelength increasing as it is in the cloudless conditions.

Some measurement results of aerosol optical thickness are shown in Figure 5. Sunward observations under clear-sky conditions and through very thin cloud layers are shown by curves 1-4; the more dense translucent clouds of upper level curves are shown by curves 5-8.

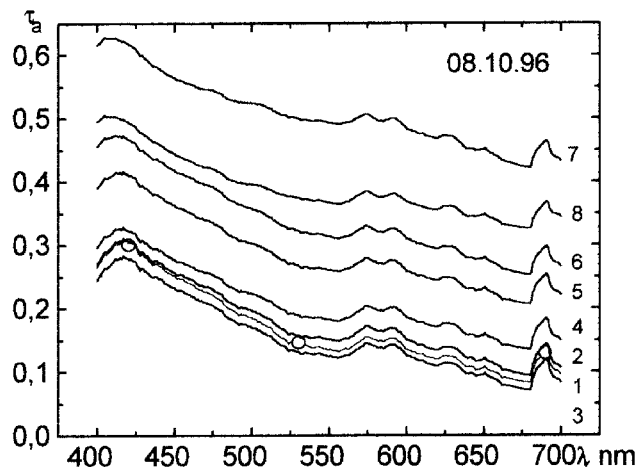


Figure 5. Spectral optical thicknesses of aerosol and translucent cloud layers obtained at afternoon on October 8, 1996. (1,2-1/Ac cuf 3-0/0; 4-6/Cc, Ci sp, Ac cuf 5, 6-1/Ci; 7-3/Ci; 8-1/Ci).

For a comparison, we have plotted the curve of the optical thickness obtained with a star and solar spectrophotometer at 1:58 p.m., October 8, 1996. As is clear from this figure, all curves have extreme s, which are antiphase to the extremes of spectral fluxes presented in Figures 4 and 5. This indicates that the observed maxima are caused by the radiation absorption by atmospheric gases. Especially, the peak at 690 nm is very pronounced, which relates to the absorption band of oxygen and water vapor.

Direct Solar Radiation

The data given in Figure 6 for the total optical depth of the atmospheric unit mass indicate that the spectral dependence of light extinction in the cloudless atmosphere and a slight cloudiness (curves 1,2) is rearranged to the neutral behavior under conditions of solid cloud cover (curve 3).

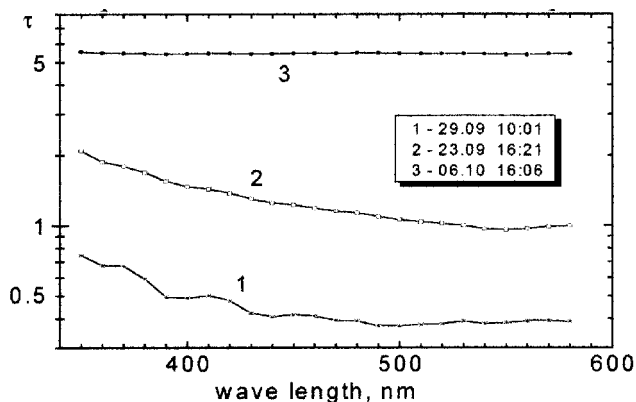


Figure 6. The atmospheric optical depths in the absence of cloudiness (1), Cs trans. (2), As op. (3).

Figure 7 shows the spectral ranges *m* (350-420nm), *n* (420-490nm) and *l* (490-560nm) denoted by vertical lines, used for investigating the spectra by means of the color coordinates method *m,n,l*, calculated as the ratio of spectral fluxes in these ranges to the net flux.

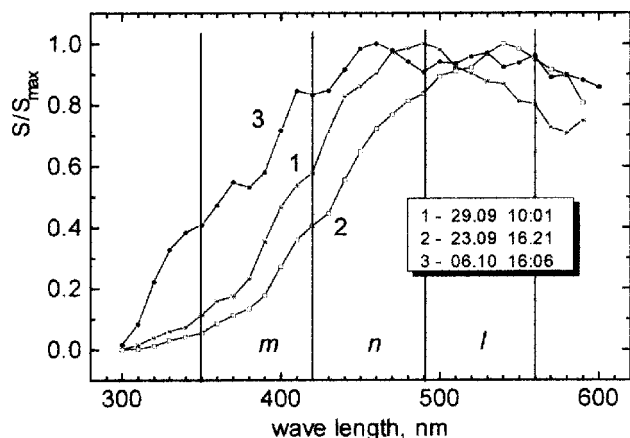


Figure 7. The typical spectra of direct solar radiation for the absence of cloudiness(1), Cs trans(2),As op(3)

Similar variability should be accounted for by a joint action of a series of factors, namely, variations of microphysical particle composition of clouds and atmospheric haze, the contribution of molecular and multiple light scattering. The total limits of variation of the optical depth in our measurements are from 0.2 to 8.

Figure 7 presents some typical characteristics of variability of direct radiation spectra S_{Σ} normalized to maximum values:

1) regularly manifested with different degree of variability maxima 370 and 420, corresponding to the extraatmospheric solar spectrum; and 2) dynamics of basic maximum, which, for solid cloud cover (curve 3), is in the spectral range of 460 to 480 nm, corresponding to extraterrestrial maximum and shifted to the <<red>> spectral range for the conditions of translucidus and clear sky (curves 1,2). The basic power exchange for all analyzed situations occurs between spectral ranges *m* and *l*.

Figure 8 illustrates the dynamics of variation of the <<net>> flux S_{Σ} (350-560nm) and relative color coordinates *m,n,l* in the cloudy (small values of S_{Σ}) and clear atmosphere over the period of measurements from September 23 to October 10, 1996. In the direct radiation spectral power the part of flux *n* (Figure 7) varies slightly (on the average, $n=0.38$, with the variation coefficient 0.1).

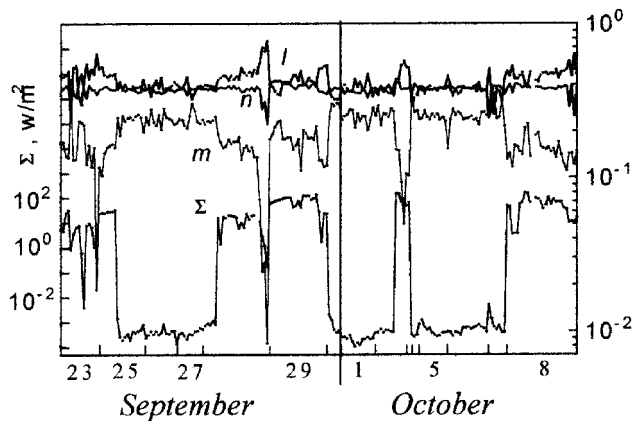


Figure 8. The total spectral flux and relative color coordinates *m,n,l* for cloudy (small values of total flux) and cloudless atmosphere.

We observe the anticorrelated character of mutual variations of color coordinates *m* and *l* and their connection with the variations of the <<net>> flux S_{Σ} .

Figure 9 gives the diagram of color coordinates (*m,l*).

Series of chromaticity points for the three basic data arrays -- <<sun>>-cloudless and light cloudiness, <<sun+cloud>>-translucidus, and <<cloud>>-solid cloud cover -- are grouped along the regression line, with the correlation coefficient about 0.93. The diagram shows the calculated points 0,1, 3, 5 for solar extraterrestrial spectrum and for molecular atmosphere with the masses $M_R=1,3,5$.

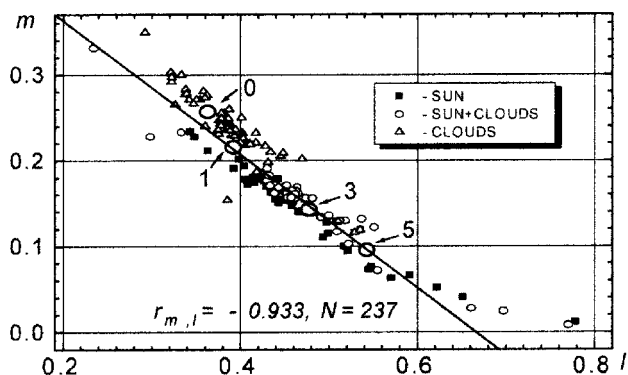


Figure 9. The points of chromaticity on the plane of color coordinates m, l for all spectra.

Conclusion

This paper describes the peculiarities of variability of solar radiation spectral fluxes in autumn 1996 in the region of the city of Tomsk. An effort has been made to follow the basic regularities of distribution of spectral brightness of direct and scattered solar radiation. Based on analysis of the data obtained during these experiments, we can draw the following conclusions:

- Continuous decrease of the spectral flux with increasing wavelength is observed in the broken cloudiness and cloudless conditions. This is a result of molecular and aerosol light scattering.
- The fine structure of spectral flux for the continuous translucent cloudiness and cloudless conditions is formed due to molecular absorption of radiation.
- For the conditions of continuous and powerful low-level cloudiness the behavior of the spectral scattered flux is of neutral type and is determined by light scattering in clouds. At the same time, the spectral structure of the flux is blurred.
- The basic power exchange for spectra of direct solar radiation occurs between spectral ranges 350-420nm and 490-560nm.
- Variability of color coordinates is determined by the joint influence of many factors, which must be taken into account at aftertreatment systematization of experimental data.

References

- Abramochkin, A. I., P. P. Vaulin, V. P. Galileiskii, A. V. Isakov, and G. V. Potemkin, 1981: Measurements of optical-meteorological atmospheric parameters with the use of laser radiation. *Stellar - solar electronic photometer*. Tomsk, Institute of Atmospheric Optics SB USSR Academy of Sciences, pp.14-19.
- Galileiskii, V. P., A. M. Morozov, and V. K. Oshlakov, 1994: Color temperature and pseudoemission properties of the atmospheric dust. *SPIE Proceedings*. Vol. 2312- 10, Rome, Italy.
- Oshlakov, V. K., 1990: Determination of cloud presence along a sighting line from photometric data. *Atmos. Optics*, **3**, 431-435.
- Serra, J., 1981: Image analysis and mathematical morphology. Academy Press, New York.